# Scanning tunneling microscopy reveals LiMnAs is a room temperature anti-ferromagnetic semiconductor

AIP | Applied Physics Letters

# Scanning tunneling microscopy reveals LiMnAs is a room temperature antiferromagnetic semiconductor

A. P. Wijnheijmer, X. Martí, V. Holý, M. Cukr, V. Novák et al.

Citation: Appl. Phys. Lett. **100**, 112107 (2012); doi: 10.1063/1.3693611
View online: http://dx.doi.org/10.1063/1.3693611
View Table of Contents: http://apl.aip.org/resource/1/APPLAB/v100/i11
Published by the American Institute of Physics.

# Scanning tunneling microscopy reveals LiMnAs is a room temperature anti-ferromagnetic semiconductor

A. P. Wijnheijmer,[1,a)] X. Martí,[2,3] V. Holý,[2] M. Cukr,[3] V. Novák,[3] T. Jungwirth,[3,4] and P. M. Koenraad[1]
[1]*COBRA Inter-University Research Institute, Department of Applied Physics, Eindhoven University of Technology, P. O. Box 513, NL-5600 MB Eindhoven, The Netherlands*
[2]*Faculty of Mathematics and Physics, Charles University in Prague, Ke Karlovu 3, 121 16 Prague 2, Czech Republic*
[3]*Institute of Physics ASCR, v.v.i., Cukrovarnická 10, 162 53 Prague 6, Czech Republic*
[4]*School of Physics and Astronomy, University of Nottingham, Nottingham NG7 2RD, United Kingdom*

(Received 1 December 2011; accepted 19 February 2012; published online 14 March 2012)

We performed scanning tunneling microscopy and spectroscopy on a LiMnAs(001) thin film epitaxially grown on an InAs(001) substrate by molecular beam epitaxy. While the *in situ* cleavage exposed only the InAs(110) non-polar planes, the cleavage continued into the LiMnAs thin layer across several facets. We combined both topography and current mappings to confirm that the facets correspond to LiMnAs. By spectroscopy we show that LiMnAs has a band gap. The band gap evidenced in this study, combined with the known Néel temperature well above room temperature, confirms that LiMnAs is a promising candidate for exploring the concepts of high temperature semiconductor spintronics based on antiferromagnets. © *2012 American Institute of Physics*. [http://dx.doi.org/10.1063/1.3693611]

The seminal paper by Dietl *et al.*[1] predicting high temperature ferromagnetism in Mn-doped III-V semiconductors triggered an intense research with the aim of integrating spin and charge electronics in one material. A number of intriguing spintronic phenomena and functionalities have been demonstrated in (Ga,Mn)As (Ref. 2); however, the Curie temperature ($T_C$) in materials with the highest attainable Mn-doping remains below room temperature.[3,4] Increasing the substitutional Mn-doping and thus increasing $T_C$ beyond the current limits is a challenge from the growth perspective, and, moreover, it is unavoidably linked with increasing the carrier density far above the common semiconductor doping levels. Mašek *et al.*[5] proposed to replace the III-V semiconductor hosts with I-II-V compounds in which there is no limit on the isovalent substitution of the group-II element by Mn, and the carrier doping can be controlled independently of the concentration of Mn. Ferromagnetism has been indeed recently demonstrated in Li(Mn,Zn)As; however, $T_C$ is still below room temperature.[6] The interest in the I-II-V semiconductors combined with the proposed concept of antiferromagnet-based spintronics[7] (recently realized in metal antiferromagnets[8]) has brought the attention to the antiferromagnetic I-Mn-V compounds, particularly LiMnAs.[9] It has been suggested that considering antiferromagnetic instead of ferromagnetic semiconductors may overcome both the limitations of the low magnetic transition temperature and high carrier doping.

Epilayers of LiMnAs have been grown by molecular beam epitaxy (MBE)[9] showing the same crystal structure as the bulk materials, known for many years as high Néel temperature ($T_N > 393$ K) compounds.[10] Despite the exhaustive characterization already presented, complemented by band-structure calculations predicting the semiconducting nature of LiMnAs, only indirect experimental evidence of a semiconductor band structure was provided. Here we report on a scanning tunnel microscopy (STM) study which evidences that LiMnAs films grown on InAs(001) substrates have a band gap.

We use an Omicron low temperature STM for our investigations, operated at 5 K. We cleave our samples in ultra high vacuum (UHV) just before the measurements, exposing a clean and atomically flat {110} surface. The tips are electro-chemically etched from polycrystalline tungsten wire. Further preparation in UHV guarantees tips with atomic resolution that are stable for many days.[11]

The sample consists of a 300 nm LiMnAs layer on a InAs substrate, grown by MBE approximately one year ago; see Ref. 9 for the details of the MBE growth. Because of the known ageing issues connected with Li containing materials, a sample from the same wafer was investigated by x-ray diffraction (XRD) in parallel with the STM experiments. A decrease of the intensity and broadening of the LiMnAs peaks, as compared to XRD measurements reported in Ref. 9, suggest a degradation of the upper part of the LiMnAs film with the free surface exposed to air. Therefore, we focused our STM analysis on the bottom part of the LiMnAs epilayer near the interface with the InAs substrate.

Figure 1 shows a cross-sectional STM topography (a) and a current image (b), obtained at the InAs/LiMnAs interface. The feed-back loop is controlled by the tunneling current, and therefore the current image contains the error information of the topography scan. It can also be interpreted as the lateral derivative of the topography. We find the InAs/LiMnAs interface at a distance of ~300 nm from the sample surface, which corresponds with the thickness of the originally grown layer. This confirms that the main damage pointed out in the XRD experiments concerns the crystal structure, probably oxidation, but not evaporation or similar

[a)]Electronic mail: a.p.wijnheijmer@alumnus.tue.nl.

 

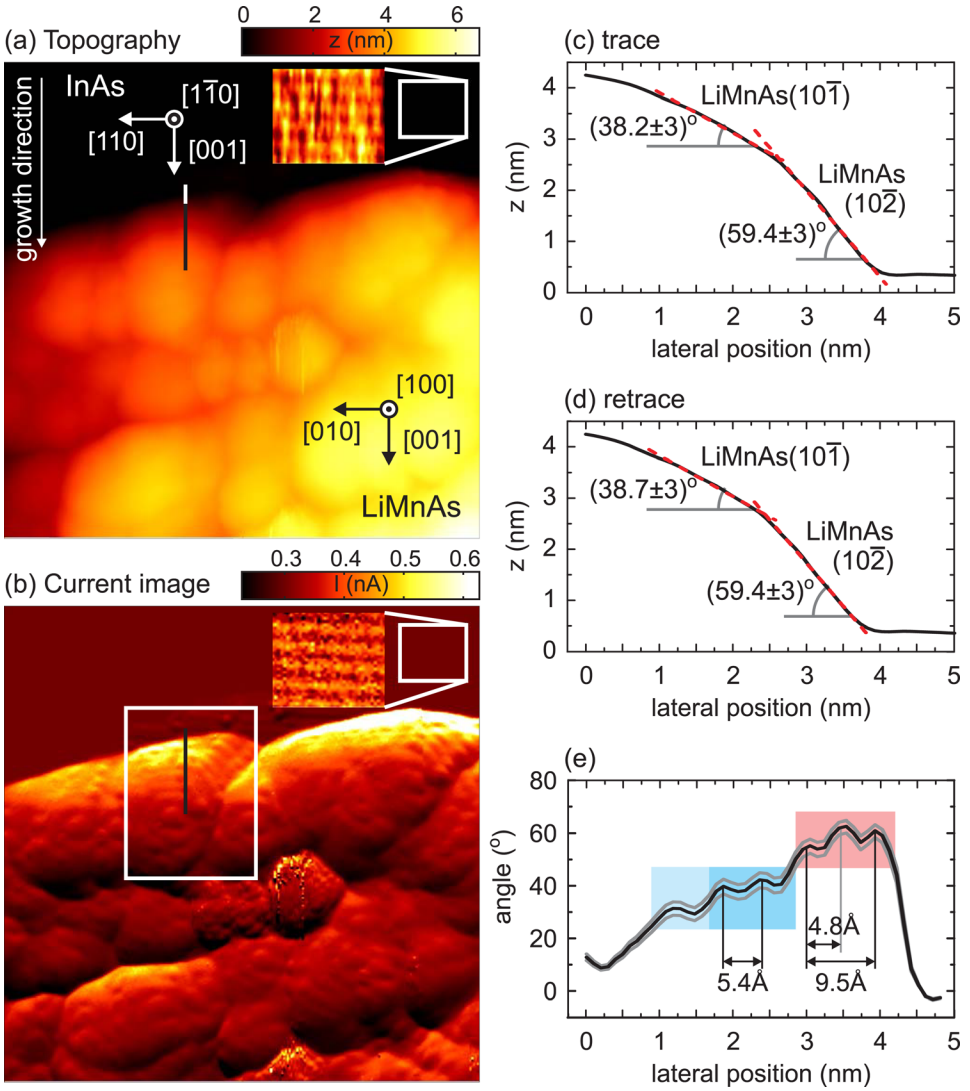


FIG. 1. (Color online) STM topography image (a) and the corresponding current image (b) at the InAs-LiMnAs interface. The setpoint was 2.1 V and 300 pA. The growth direction is indicated. The fast scanning direction is from top to bottom and the slow scanning direction from right to left. (c) and (d) line section through the image in (a), for the trace and retrace scan, respectively. (e) Lateral derivative of the topography section in (c) expressed in an angle.

removal of the layer. The growth direction is indicated in the image. The natural cleavage plane of InAs is any of the {110} planes. In practice, we always expose the (110) or (1 $\bar{1}$ 0) plane, because we cleave perpendicular to the growth direction [001]. The atomically flat InAs(1 $\bar{1}$ 0) surface is clearly seen in Fig. 1, and the atomic corrugation is visible (inset). The cleavage on the LiMnAs layer is not flat and shows a very rough landscape with a scale of up to 6 nm. This is caused by the non parallel arrangement of the natural cleavage planes of InAs and LiMnAs. The current images (Fig. 1(b)) clearly reveal a periodic oscillation modulated on the sample topography. We will show in the following that this periodicity corresponds to the LiMnAs(001) material.

As shown in Fig. 2(a), LiMnAs has a tetragonal crystal structure. The unit cell of LiMnAs is rotated by 45°, thus becoming almost perfectly coincidence-site lattice matched to the InAs substrate.[9] The Miller indices of both materials are shown in the image. Note that InAs is cubic and has a lattice constant of 6.06 Å along all directions. However, LiMnAs is compressed along the [001] direction. The lattice constant of LiMnAs along the [100] and [010] direction is 4.28 Å and along the [001] direction 6.16 Å. To avoid confusion in the basis used, both the compound and the Miller indices will always be indicated.

A key requirement for a natural cleavage plane is that it has to be non-polar. In case of LiMnAs it means that in the surface the ratio between Li:Mn:As should be 1:1:1. There are several planes that fulfill this requirement, for example, the LiMnAs(100) and (101) planes. The STM image reveals several facets. We identify which facet corresponds to which plane by comparing the angle between the facet and the LiMnAs(100) plane, which is equivalent to the flat InAs(1 $\bar{1}$ 0) surface. The line sections through the topography, taken parallel to the [001] direction, are shown in Figs. 1(c) and 1(d), for the trace and the retrace scan, respectively. For the trace scan the fast scanning direction was from bottom to top; for the retrace scan it was from top to bottom. Figure 1(e) corresponds to the lateral derivative of the topography section in Fig. 1(d), expressed in an angle. The topography section reveals at least two facets, which we locally fit by linear functions, in order to extract the angles between these facets and the LiMnAs(100) plane. Note that there is a strong signal in the current image, indicating that the feedback loop has not completely stabilized due to the steep facets. However, this effect is opposite for the trace and the retrace scan, and the angles obtained from the trace and retrace scan differ by less than 0.5° (see Figs. 1(c) and 1(d)). We find a take off angle $(59.4\pm3)^\circ$ for the steep part and

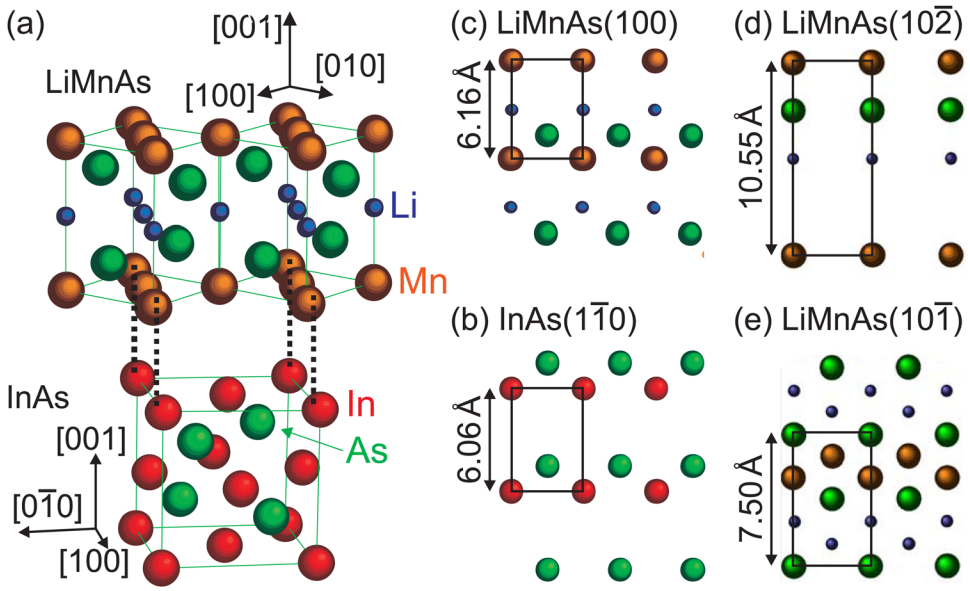


FIG. 2. (Color online) (a) Crystal structure of LiMnAs and InAs. The Miller indices of both materials are indicated. (b)-(e) Atomic arrangement of several non-polar planes.

$(38.5\pm3)^\circ$ for flatter part. The relatively large error originates from a 10% uncertainty in the calibration of the *z*-piezo. We infer that the steep part is LiMnAs(1 0 $\bar{2}$) plane and the flatter part is LiMnAs(1 0 $\bar{1}$). The nominal angles for these planes are 54.3° and 34.8°, respectively,[15] which is consistent with the measured take off angles. These two planes are indeed non-polar, as shown in Figs. 2(c)–2(e). We allowed a 0.2 Å tolerance to produce the planes, i.e., atoms that are 0.2 Å away from the plane are still shown. For comparison, the InAs(1 $\bar{1}$ 0) plane is also shown.

We can furthermore compare the inter-atomic distances, which is best visible in the derivative of the topography (Fig. 1(e)). From the STM measurement we obtain 4.8 Å for the LiMnAs(1 0 $\bar{2}$) plane (the steep part) and 5.4 Å for the LiMnAs(1 0 $\bar{1}$) plane (the flatter part). However, in STM a top view is measured. We thus have to correct them for the take off angles of the facets in order to compare it with the nominal values. We find $(9.44\pm1.1)$ Å for the LiMnAs(10 $\bar{2}$) plane and $(6.92\pm0.4)$ Å for the LiMnAs(1 0 $\bar{1}$) plane. These are slightly smaller than the nominal values of 10.55 and 7.50 Å obtained from XRD. This is probably due to surface reconstructions or due to thermal expansion, as the XRD measurements are performed at room temperature and the STM measurements at 5 K.

Having determined the facets and proven that it is crystalline LiMnAs, we perform scanning tunneling spectroscopy (STS) on this area in order to extract an estimate of the band gap. We take $I(V)$ spectra on a grid of 256 px × 256 px. Each spectrum runs from −2 to 2.1 V in 250 voltage steps. The differential conductance is obtained by numerically differentiating the $I(V)$ curve after the actual measurement. The differential conductance d $I$/d $V$ corresponds to the local density of states (LDOS) when a constant tip-sample distance ($z_{tip}$) is assumed.

Figure 3(a) shows a lateral d $I$/d $V$ image at −1.54 V, obtained at the same area of the sample as is shown in Fig. 1. The zoom of the cyan rectangle in (b) shows the STM current map to facilitate the comparison of the facets. In Fig. 3(c), four d $I$/d $V$ curves are shown. One is obtained at the InAs substrate (solid black, averaged over the black rectangle in Fig. 3(a)) and the other three on the LiMnAs layer. The red dotted lines are obtained on the LiMnAs(1 0 $\bar{2}$) facet (averaged over the red dotted rectangle in Fig. 3(b)), the green dash-dotted on the LiMnAs(1 0 $\bar{1}$) facet (averaged over the green dash-dotted line in Fig. 3(b)), and the blue dashed on a different LiMnAs facet (averaged over the blue dashed rectangle in Fig. 3(b)). From these curves, we can extract the width of the band gap. We measure the width of the band gap at d $I$/d $V = 0.1$ pA/V and at d $I$/d $V = 0.5$ pA/V, and we average these two values. The difference is a measure of the error. We find $(650\pm50)$ meV for InAs, $(630\pm100)$ meV for LiMnAs(1 0 $\bar{2}$), $(810\pm50)$ meV for LiMnAs(1 0 $\bar{1}$), and $(390\pm50)$ meV for the last LiMnAs facet. The obtained value for InAs is larger than the bulk value of 418 meV. This is due to tip-induced band bending effects,[12–14] which lead to an overestimation of the band gap in STS measurements, typically by a few hundred meV. The same effect plays a role on LiMnAs. However, it is difficult to estimate whether the effect is smaller, similar, or larger than on InAs. It is therefore difficult to give a lower limit of the width of the band gap. The difference between the band gaps on the three LiMnAs facets might be due to surface states that move into the band gap. The different surfaces have possibly different surface reconstructions, which can affect the positions of the surface states. Furthermore, STS shows the smallest band gap, and in case the material has an indirect band gap, optical absorption measurements will give a higher value. All these considerations make it difficult to give a quantitative estimate of the band gap. However, from these STS measurements we can unambiguously conclude that LiMnAs has a finite band gap. Figure 3(d) shows a d $I$/d $V$ section along the black line in Figs. 3(a) and 3(b). The band gap on the InAs substrate and the LiMnAs region are clearly visible and do not fluctuate with position.

To summarize, we have performed cross-sectional STM and STS on epitaxially grown LiMnAs. We found crystalline

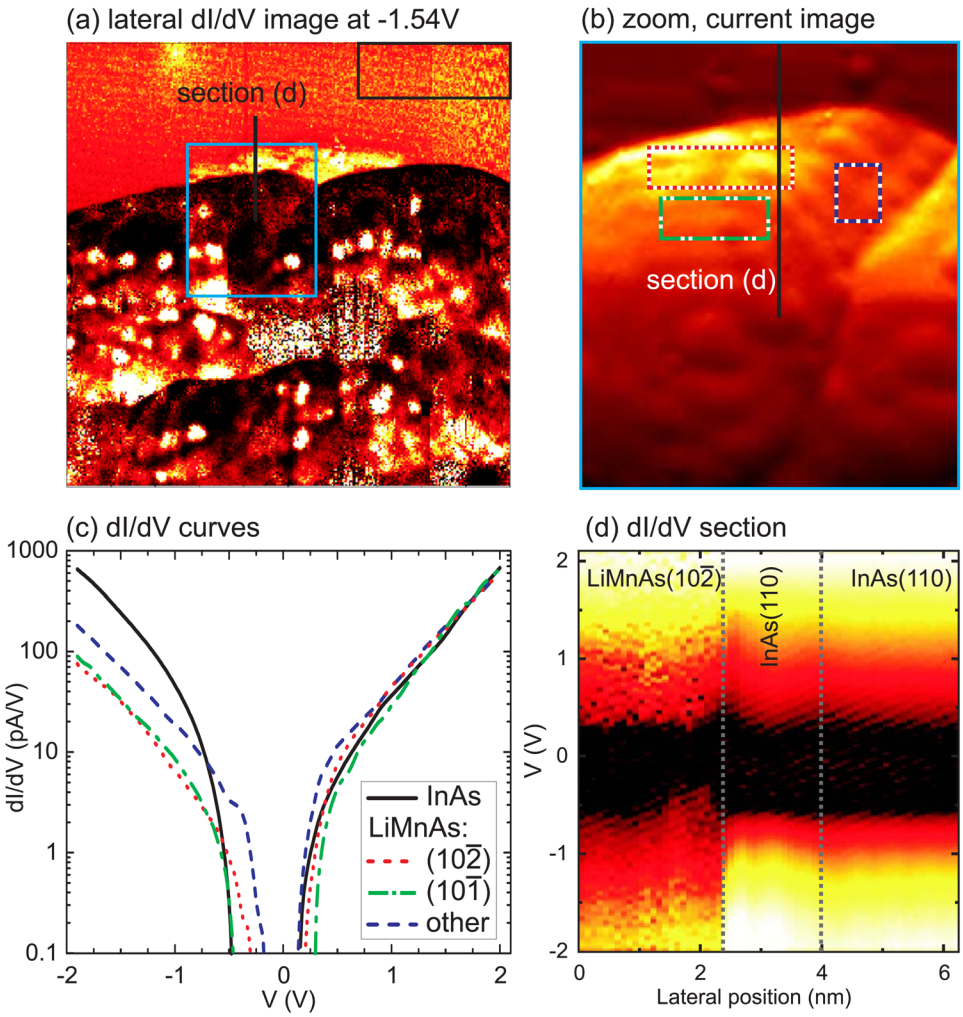


FIG. 3. (Color online) (a) Lateral d $I$/d $V$ image at −1.54 V, obtained at the same area of the sample as shown in subset (b) and in Fig. 1. (c) Spectra on InAs and on LiMnAs at the positions indicated in (b), showing the band gap. (d) Line section along the line in (b), showing the variation of the band gap with position.

LiMnAs regions close to the InAs/LiMnAs interface, which we confirmed by identifying the facets and comparing the inter-atomic distances. STS on the same area revealed a band gap. This prove of the existence of a finite band gap, combined with the known Néel temperature well above room temperature, confirms that LiMnAs is a promising candidate for exploring the concepts of high temperature semiconductor spintronics based on antiferromagnets.

This work was supported by the EU Grant FP7-214499 NAMASTE and ERC Advanced Grant 268066, from Czech Republic Grants AV0Z10100521, LC510, P204/11/P339, and Preamium Academiae. The authors acknowledge support from J. K. Garleff.

[1]T. Dietl, H. Ohno, F. Matsukura, J. Cibert, and D. Ferrand, Science **287**, 1019 (2000).
[2]T. Dietl, D. D. Awschalom, M. Kaminska, and H. Ohno, Semicond. Semimetals **82**, ix–xiii (2008).
[3]K. Olejník, M. H. S. Owen, V. Novák, J. Mašek, A. C. Irvine, J. Wunderlich, and T. Jungwirth, Phys. Rev. B **78**, 054403 (2008).
[4]M. Wang, R. P. Campion, A. W. Rushforth, K. W. Edmonds, C. T. Foxon, and B. L. Gallagher, Appl. Phys. Lett. **93**, 132103 (2008).
[5]J. Mašek, J. Kudrnovský, F. Máca, B. L. Gallagher, R. P. Campion, D. H. Gregory, and T. Jungwirth, Phys. Rev. Lett. **98**, 067202 (2007).
[6]Z. Deng, C. Q. Jin, Q. Q. Liu, X. C. Wang, J. L. Zhu, S. M. Feng, L. C. Chen, R. C. Yu, C. Arguello, T. Goko *et al.*, Nat. Commun. **2**, 422 (2011).
[7]A. B. Shick, S. Khmelevskyi, O. N. Mryasov, J. Wunderlich, and T. Jungwirth, Phys. Rev. B **81**, 212409 (2010).
[8]B. G. Park, J. Wunderlich, X. Marti, V. Holy, Y. Kurosaki, M. Yamada, H. Yamamoto, A. Nishide, J. Hayakawa, H. Takahashi, *et al.*, Nature Mater. **10**, 347 (2011).
[9]T. Jungwirth, V. Novák, X. Martí, M. Cukr, F. Máca, A. B. Shick, J. Mašek, P. Horodyská, P. Němec, V. Holý, *et al.*, Phys. Rev. B **83**, 035321 (2011).
[10]W. Bronger, P. Müller, R. Höppner, and H. U. Schuster, Z. Anorg. Allg. Chem. **175**, 539 (1986).
[11]J. Garleff, M. Wenderoth, K. Sauthoff, R. Ulbrich, and M. Rohlfing, Phys. Rev. B **70**, 245424 (2004).
[12]R. M. Feenstra and J. A. Stroscio, J. Vac. Sci. Technol. B **5**, 923 (1987).
[13]R. M. Feenstra, J. Vac. Sci. Technol. B **21**, 2080 (2003).
[14]N. Ishida, K. Sueoka, and R. M. Feenstra, Phys. Rev. B **80**, 075320 (2009).
[15]$\tan^{-1}(4.28/6.16) = 34.8°$ and $\tan^{-1}(2 \cdot 4.28/6.16) = 54.3°$.